Traffic 2008; **9:** 1283–1298
Blackwell Munksgaard

doi: 10.1111/j.1600-0854.2008.00762.x

The Vaccinia Virus F11L Gene Product Facilitates Cell Detachment and Promotes Migration

Ivonne Morales[1], Maria Alejandra Carbajal[1], Stefan Bohn[1], Daniela Holzer[1], Sayuri E. M. Kato[2,3], Frederico A. B. Greco[2], Nissin Moussatché[2] and Jacomine Krijnse Locker[1,*]

[1]EMBL, Cell Biology and Biophysics Program, Meyerhofstrasse 1, 69117 Heidelberg, Germany
[2]Laboratorio de Biologia Molecular de Virus, Instituto de Biofisica, Carlos Chagas Filho, CCS, UFRJ, Rio de Janeiro, RJ 21941-902, Brasil
[3]Current address: Department of Molecular Biology, Princeton University, Princeton, NJ 08544-1014, USA
**Corresponding author: Jacomine Krijnse Locker, krijnse@embl.de*

We previously showed that infection with vaccinia virus (VV) induces cell motility, characterized by contractility and directed migration. Motility is temporally regulated because cells are motile immediately after infection, whereas late in infection motility ceases and cells resettle. Motility and its cessation are accompanied by temporal rearrangements of both the microtubule and the actin networks. Because the F11L gene has previously been implicated in VV-induced migration, we now explore the role of F11L in contractility, migration, the cessation of motility and the cytoskeletal rearrangements. By live cell imaging using a VV that lacks an intact F11L gene, we show that F11L facilitates cell detachment and is required for migration but not for contractility. By light microscopy, F11L expression induces a remodeling of the actin, but not the microtubule, network. The lack of migration correlates with smaller plaques, indicating that this process facilitates cell-to-cell spreading of VV. Late in infection, when motility ceases, cells re-establish cell-to-cell contacts in an F11L-independent manner. We finally show that VV-induced motility and its cessation correlate with a temporal regulation of the guanosine triphosphatase RhoA as well as the expression levels of F11L during the infectious cycle.

Key words: cell migration, F11L, microtubules, modified vaccinia virus Ankara, poxvirus

Received 1 May 2007, revised and accepted for publication 7 May 2008, uncorrected manuscript published online 9 May 2008, published online 18 June 2008

Cell migration is an essential cellular process required for wound healing, embryonic tissue development and movement of cancer cells. In most cell types, migration involves the regulation of both microtubule and actin dynamics and is controlled by small guanosine triphosphatases (GTPases) of the Rho family (reviewed in 1–8). Generally, the GTPase rac-1 is involved in the formation of an actin-rich lamellipodia at the leading edge of the migrating cell. CDC42 generates filopodia that protrude from the lamellipodia and may aid in the polarization of the cell in the direction of migration. RhoA regulates cell adherence and promotes detachment at the rear of the cell, thus enabling forward movement.

Being strictly obligatory intracellular pathogens, viruses exploit the host-cell machinery to produce infectious progeny. Thus, various steps of the life cycle of the large DNA virus, vaccinia virus (VV), a member of the poxviridae, interact with membranes and the cytoskeleton (9,10). These interactions are accompanied by a remodeling of membranes and the cytoskeleton that likely facilitate the VV life cycle (9,11). Thus, VV induces cell motility early in infection that is characterized by phases of cell migration alternated by cellular contractions (12,13). Motility is accompanied by dramatic rearrangements of both microtubules and actin (11,13). Motility also unexpectedly contributes to the perinuclear accumulation of the viral DNA replication sites; these sites are formed in the cellular periphery, and live cell imaging implied that cytoplasmic forces that accompany motility arranges them around the nucleus in a microtubule-dependent (but dynein-independent) manner (13). An important control for these experiments was the attenuated VV-modified vaccinia virus Ankara (MVA) in which about one third of the VV genes are deleted or inactive (14,15). This virus does not induce motility (13,16) and cytoskeletal rearrangements (11), and its replication sites do not accumulate around the nucleus (13).

The F11L gene of VV has previously been implicated in VV-induced cell motility. This viral protein has been proposed to regulate the GTPase RhoA, thus enabling cell detachment (16). To what extent F11L was responsible for migration, contractility or the rearrangement of microtubules and actin was not investigated. A recent study suggested that F11L alters the dynamics of microtubule ends located in the cellular periphery late in infection when motility ceases and cells resettle (17).

Poxviruses are characterized by a highly programmed life cycle that occurs entirely in the cellular cytoplasm (18). The early phase consists of virus entry, early gene transcription and cytoplasmic DNA replication and is accompanied by cell motility (13). The late phase consists of the assembly and egress of progeny virus and cessation of cell motility. Newly synthesized viruses leave cells using both microtubules and actin tails, a process that facilitates cell-to-cell spread of the virus (10).

In this study, we wished to explore the role of F11L in cell motility (this is, migration and contractility), cytoskeletal rearrangements that accompany motility and the viral life cycle. Using a VV that lacks an intact F11L gene, we show that F11L induces actin rearrangements and promotes cell migration. In contrast, F11L is not required for contractility and the microtubule changes. We show that the expression of F11L and the activity of RhoA are temporally regulated, providing an explanation for the time-dependent cell motility. Finally, the lack of F11L expression coincides with a smaller plaque phenotype, indicating that migration also contributes to cell-to-cell spread of VV.

Results

F11L induces cell migration

Small-interfering RNA (siRNA)-mediated knockdown of F11L was previously shown to block VV-induced migration in a wound-healing assay (16). To explore the role of F11L in migration, contractility and cessation of migration, we first expressed green fluorescent protein (GFP)-tagged F11L in MVA-infected cells because this virus does not induce motility. As before, we imaged several fields of subconfluent cells from 1- to 12-h postinfection using a program that enabled us to follow more than one location in the cell culture dish (19). Movies of wild type (wt)-VV-infected cells showed that they round up and lose cell–cell contacts, similar to our previous results (13). The cells undergo repeated contractions/blebbing and nuclear movement (that we refer to as 'contractility'), and a subset of cells undergo directed migration (Movie S1). From about 7-h postinfection, all motile activities (contractility and migration) cease; the cells reflatten and adopt a multibranched morphology that likely provides multiple substrate attachment sites. In contrast, movies of MVA-infected cells showed none of these motile activities (Movie S2) as shown before (11,13).

When we analyzed the effect of GFP-tagged F11L expression in MVA-infected cells (Movie S3), a GFP signal could be detected from about 4-h postinfection onwards. From about 6-h postinfection, a subset of the GFP-F11L-expressing cells were seen to detach from their neighbors (cell '1' in Figure 1A,B) to form a lamellipodium (cell '1' in Figure 1B,E) and to move through the monolayer (cell '1' in Figure 1A–F, Movie S3). Unlike VV-infected cells, this GFP-F11L-induced migration seen between 6- to 8-h postinfection was not alternated by contractility (Movie S3). Instead, GFP-expressing cells seemed to glide through the subconfluent monolayer of nonexpressing cells (Movie S3, cell '1' in Figure 1A–F). From about 8-h postinfection onwards, migration ceased; however, in contrast to VV, F11L-expressing MVA-infected cells did not spread out and formed a multibranched appearance. Instead, they rounded up (compare cells '1–3' in Figure 1A with the same cells in Figure 1G–P), occasionally displayed blebbing and contractions (cells '1' and '2' in Figure 1J–P, Movie S3) and typically formed several long protrusions with which they contacted neighboring cells [see also Valderrama et al. (16)]. Thus, whereas in VV-infected cells the migration phase is accompanied by contractility, F11L-expressing MVA-infected cells displayed migration (between 6- to 8-h postinfection) that was not alternated by contractility.

Analyses of a total of 50 cells per condition (derived from three independent live cell imaging experiments) showed that contractility (that is blebbing, contractions and nuclear movement) was very prominent in wt-VV-infected cells as more than 80% of the cells displayed at least one of the three contractile activities. Migration (movement of more than one cell length over the recorded time) was detected in about 30–40% of the cells, consistent with previous results [(13); data not shown]. As described before (13), MVA-infected cells displayed no motile activities, whereas F11L-expressing MVA-infected cells induced migration in about 20% of the expressing cells. Less than 5% of F11L-positive MVA-infected cells showed contractility (blebbing and contractions), and these activities were recorded at later times postinfection after migration had ceased (see previously).

We conclude that in MVA-infected cells, F11L is able to induce migration that, unlike wt-VV infection, is not alternated by phases of contractility.

F11L is not required for cell contractions

To confirm that F11L was sufficient for cell migration, we made use of a VV strain that lacks an intact F11L gene by introducing two stop codons at amino acids 15 and 75 (20). Western blot analysis showed that this virus failed to express F11L (Figure 2C). By live cell imaging, upon infection with this virus, cells were seen to undergo repeated blebbing and contractions similar to wt-VV-infected cells (Figure 2A, panels a–h, Movie S4). Although cells formed a lamellipodium (Figure 2A, panels b and f), they were unable to detach from their neighbor and to move away. The cells were displaced from their original position in the dish (compare Figure 2A panel b with i, Movie S4), but this displacement did not resemble typical migration. Instead, the repeated phases of blebbing and contractions seemed to result in a gliding along the substrate of a group of cells, generally over a short distance. Quantification of the motility in VVΔF11L-infected cells showed that contractions were as frequent as with wt-VV (around 85%), but migration was never observed (data not shown).

Similar to wt-VV-infected cells, from about 7-h postinfection with VVΔF11L, all motile activities ceased. This cessation typically coincided with a different cellular activity; infected cells grew plasma membrane extensions with which they established new cell-to-cell contacts (Figure 2A, panels h and i, Figure 2B, panels a–e, Movie S4). Although VVΔF11L-infected cells flattened out, they did

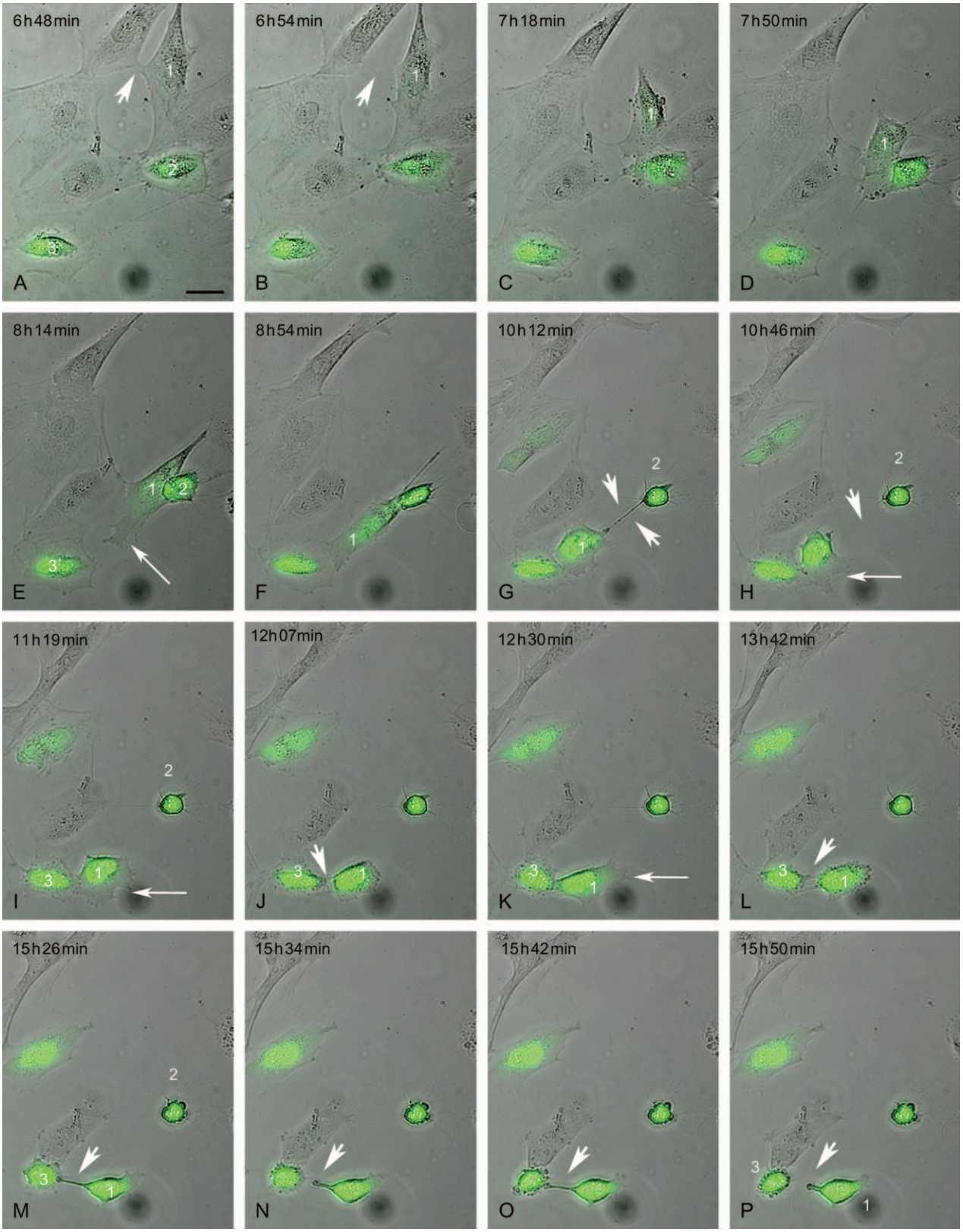

Figure 1: Legend on next page.

not adopt the multibranched morphology that typically accompanies the late phase of wt-VV infection.

The live cell imaging analyses of VVΔF11L confirms that F11L is required for migration but not for contractility, implying that both processes may have different regulatory mechanisms. The imaging of VVΔF11L also implied that F11L was not required for the cessation of the collective motile activities or for the formation of new cell-to-cell contact observed late in infection.

F11L contributes to cell-to-cell spread of VV

Previous results suggested that F11L was required for virion formation because siRNA-mediated knockdown of F11L affected virion assembly, as assessed by electron microscopy (EM) (16). The fact that we were able to grow infectious virus that lacked an intact F11L gene seemed at odds with this result. Indeed, in a one-step growth curve, the production of intracellular infectious progeny of VVΔF11L was comparable to wt-VV (Figure 3A). Moreover, when analyzing infected cells by EM, many spherical immature virions (IVs), mature viruses (MVs) and intracellular enveloped viruses (IEVs) were observed with both VV and VVΔF11L (Figure S1A–I). Quantification of the different virus forms by EM revealed no major difference between the two viruses (Table 2). Interestingly, however, although VVΔF11L and wt-VV displayed similar amounts of virus-tipped actin tails (at 8-h postinfection, 30–40% of the infected cells displayed an average of five actin tails per cell under our infection conditions; data not shown), VVΔF11L yielded significant smaller plaques compared with wt-VV (Figure 3B).

These collective data show that F11L is not required for virion assembly. The small plaque phenotype of VVΔF11L also provides evidence that VV-induced cell migration contributes to cell-to-cell spread of infectious virus.

RhoA activation and F11L expression are regulated over the time of infection

Our collective data suggested that F11L may be required for cell detachment but not for cell attachment late in infection. A role in cell adhesion seemed consistent with the proposed role of F11L in regulating the GTPase RhoA (16) because this GTPase regulates cell adherence. However, our observation that cells detached and then made new cell-to-cell contacts early and late in infection, respectively, implied that the activity of F11L and/or RhoA must be temporarily regulated.

We therefore first analyzed the level of activated RhoA throughout the infection, previously shown to be significantly reduced when analyzed at one time postinfection only (16). Whereas infection did not affect the total level of RhoA (Figure 4A, lower panel), levels of activated RhoA were significantly reduced at 3-h postinfection but regained uninfected control levels at 8-h postinfection (Figure 4A). This decrease in activated RhoA seen early in infection was dependent on F11L expression because it was not observed upon infection with VVΔF11L. We then analyzed the expression levels of F11L over the time of infection. Although VV genes carrying an early VV promoter are synthesized early in infection only, some of their gene products can be remarkably stable over the time of infection [see for instance Doglio et al. (21)]. F11L expression, however, typically decreased over time; it was greatly reduced at 12-h postinfection and could no longer be detected at 24-h postinfection (Figure 4B). Thus, we propose that the regulation of the F11L expression may underlie the time-dependent (in)activation of RhoA.

F11L is required to induce actin, but not microtubular, rearrangements

Because F11L was required for migration but not for contractility, we now asked to what extent F11L expression contributed to the typical cytoskeletal rearrangements that accompany wt-VV infection. We also hoped to establish a link between modified actin and microtubules and contractility and migration, respectively.

Whereas in uninfected PtK2 cells actin fibers cross the entire cell surface (Figure 5A), upon infection with VV, actin concentrates at the rims of the cell, leaving the more central parts free of actin fibers [Figure 5D; see Schepis et al. (11)]. Microtubules concentrate around the nucleus (Figure 5E), whereas in uninfected cells, they reach out into the cellular periphery (Figure 5B). These cellular rearrangements are also accompanied by a significant decrease in the cell surface area on the substrate, as shown before (11).

In contrast, upon infection with MVA, actin displays a pattern that is indistinguishable from uninfected controls

Figure 1: Still images of Movie S3 of MVA-infected F11L-GFP-transfected cells. PtK2 cells were infected with MVA and transfected with GFP-F11L, followed by live cell imaging as described in Movie S3. The still images (A–P) are taken from one field of Movie S3 with three GFP-F11L-expressing cells indicated 1–3. Cell '1' is seen to detach [compare (A) with (B), the arrowhead indicates connection between two cells in (A) and the loss of this contact in (B)] and then starts to move [compare its position in (A–F)]. In (E), cell '1' displays a lamellipodium (long arrow). At later times postinfection, the transfected cells are seen to form thin long connections [arrowheads in (G)] and round up [compare cell '2' in (A) with cell '2' in (G) or cell '1' and '3' in (A) with cells '1' and '3' in (I–P)]. The thin connections are then either lost [compare (G) with (H) for cell '2', indicated with arrowheads) or repeatedly lost and re-established as shown by cells '1' and '3' in the sequence (J–P) (arrowheads indicate connections or the loss of connections). At later times, transfected cells also display blebbing [for instance, cell '1' in (J) and (L) and cell '3' in (N–P)]. The times postinfection are indicated at the top left of each still image. Bar in (A), 30 μm.

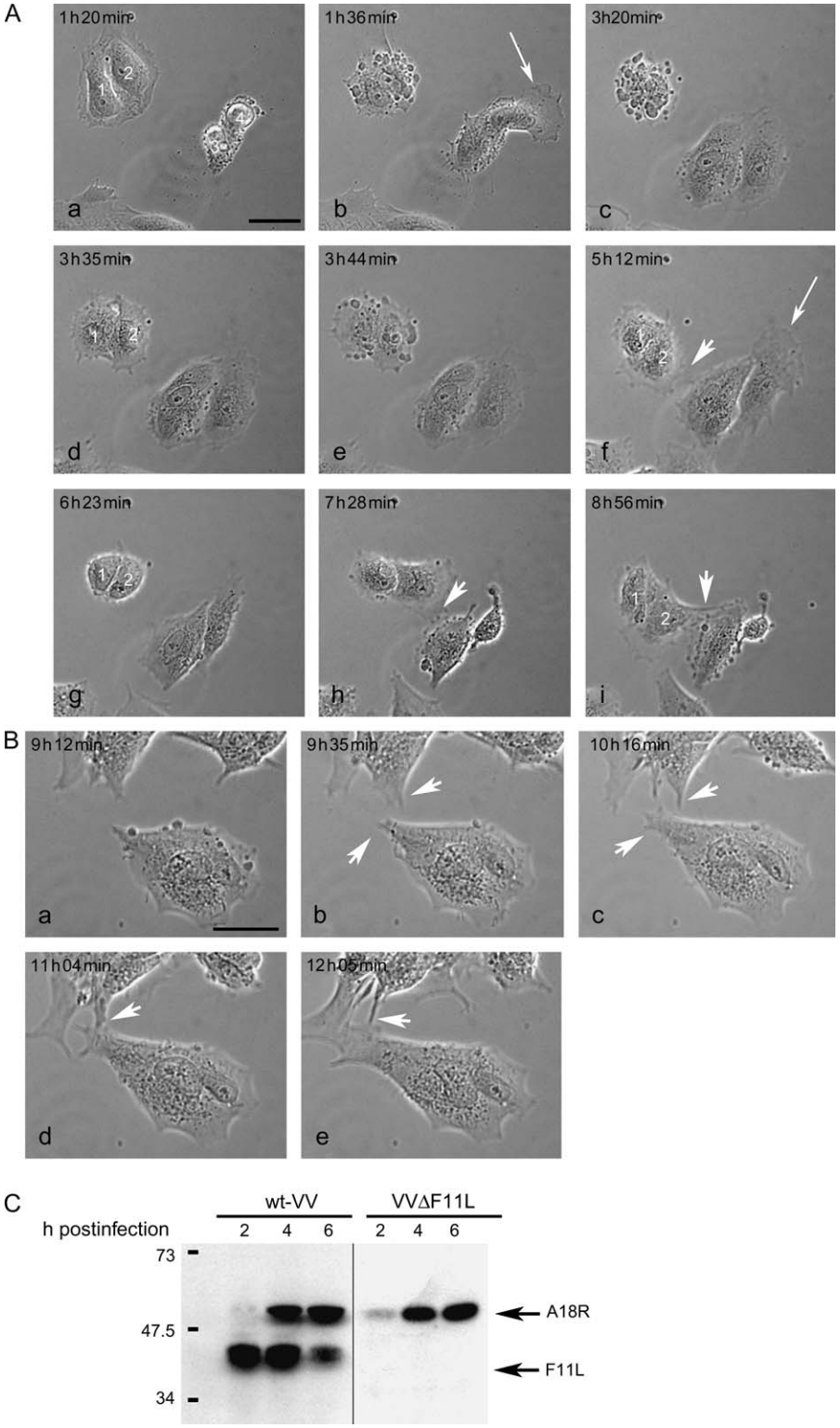

Figure 2: Still images of Movie S4 of VVΔF11L-infected cells. PtK2 cells were infected with VVΔF11L and subjected to live cell imaging as described in Figure 5. The images are taken from Movie S4 and represent typical motile events seen upon infection with this virus. The series in (A) shows the events that occur early in infection. Cells undergo repeated blebbing and contractions [compare cells '1' and '2' in a and b, in c–e and in g–h panels]. Cells also transiently make lamellipodia thin arrow in b, but they are unable to detach from each other. The series in (B) represents the typical 'late' events; cells are seen to extend plasma membrane protrusions with which they gradually establish contact with neighboring cells [compare panel a with panel e, the extensions and connections are indicated with arrowheads]. At this stage of infection, blebbing and contractions are not seen. In (A), a cell attachment event is also seen in series (A) at f and i panels (arrowheads). The times postinfection are indicated at the top left of the images. Bars in (A), panel a and (B) panel a, 30 μm. In (C), western blot analysis of wt-VV and VVΔF11L shows that F11L is not detectable in the latter virus. A18R is a VV gene expressed throughout the infection and was used as a loading control.

[Figure 6B; (11)]. Expression of GFP-F11L in MVA-infected cells induced an actin pattern that resembled VV-infected cells in which actin concentrated at the cell borders and was absent from the central parts of the cell (compare Figure 5D with Figure 6B). However, F11L expression was unable to induce the typical retracted microtubular phenotype that accompanies VV infection (Figure 6E). Infection with VVΔF11L confirmed that F11L promoted actin but not

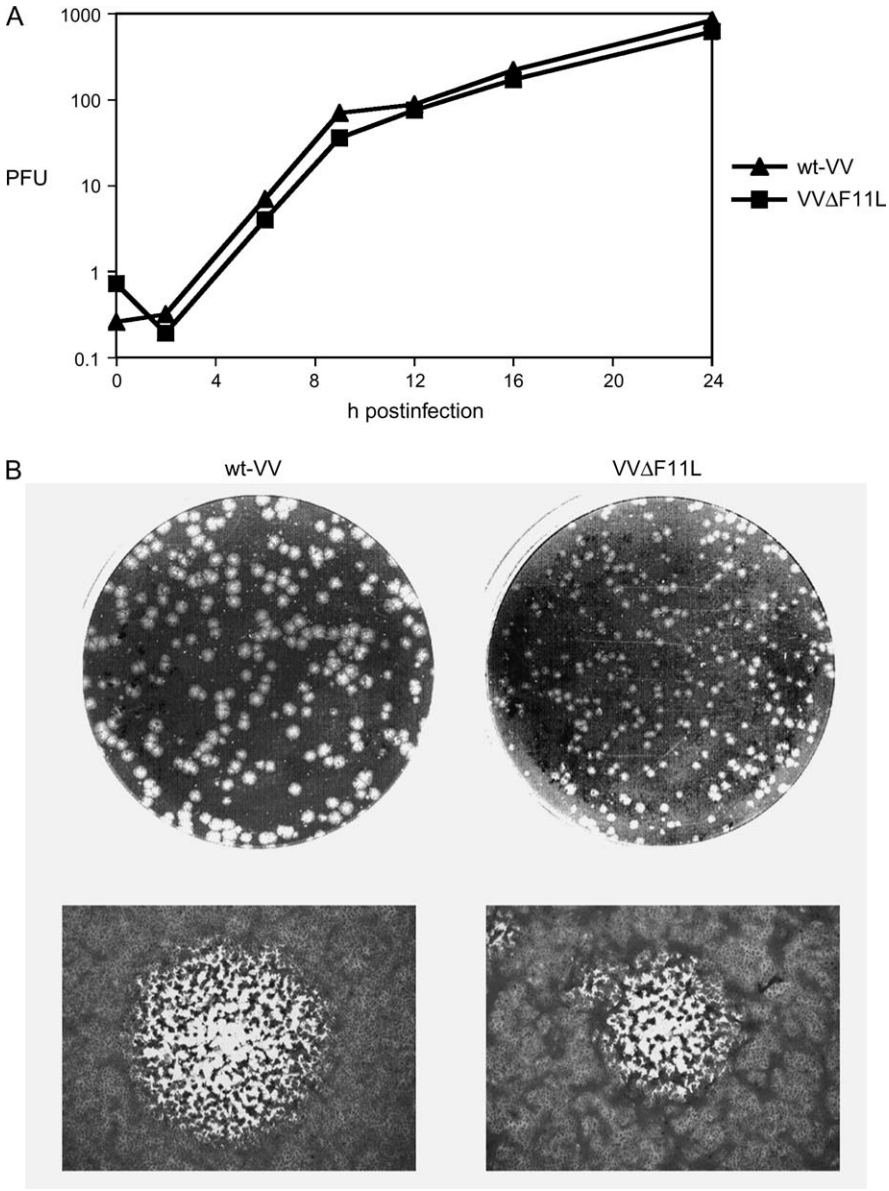

Figure 3: F11L contributes to cell-to-cell spread of VV. In (A), BSC40 cells grown in a 3.5-cm dish were infected at an MOI of 10 for 30 min with either wt-VV or VVΔF11L. The cells were harvested at the indicated times postinfection and the infectivity determined by plaque titration. PFU, plaque forming units contained in the total cell lysate. (B) shows the size of the plaque obtained with either wt-VV or VVΔF11L. The upper panel shows an overview, and the lower panel a higher magnification of one plaque emphasizing the size difference.

microtubular rearrangements; upon infection with this virus, actin resembled the uninfected pattern (Figure 6G), whereas the microtubules were concentrated around the nucleus similar to wt-VV (Figure 6H).

We then estimated the percentage of cells with a loss of central actin fibers or with collapsed microtubules (Figure 6J,K). The loss of central actin fibers was very prominent (around 85%) in wt-VV-infected cells and occurred with relatively low frequency (15%) with MVA (Figure 6J). The expression of F11L in MVA-infected cells induced a significant increase in cells without central actin fibers (from 15 to 65%), whereas this percentage was only around 30% upon infection with VVΔF11L (Figure 6J). Microtubule collapse occurred equally well in wt-VV- and VVΔF11L-infected cells (around 80–90% of the cells), whereas this was not a prominent phenotype in MVA-infected cells and this was irrespective of F11L expression (5 and 15% with or without F11L expression, respectively; Figure 6K).

Upon infection with wt-VV, all motile activities cease at later times postinfection (13). This coincides with a reflattening of the cells that progressively adopt a multibranched morphology with a thin actin layer following the cell borders [Figure 7A,E; (11)]. At later times of VVΔF11L infection, actin resembled the pattern seen at 4-h postinfection with this virus; although infected cells also reflattened, they did not adopt a multibranched morphology typically seen during wt-VV infection (Figure 7B). In contrast, GFP-F11L-expressing MVA-infected cells adopted a morphology described above, with a rounded cell

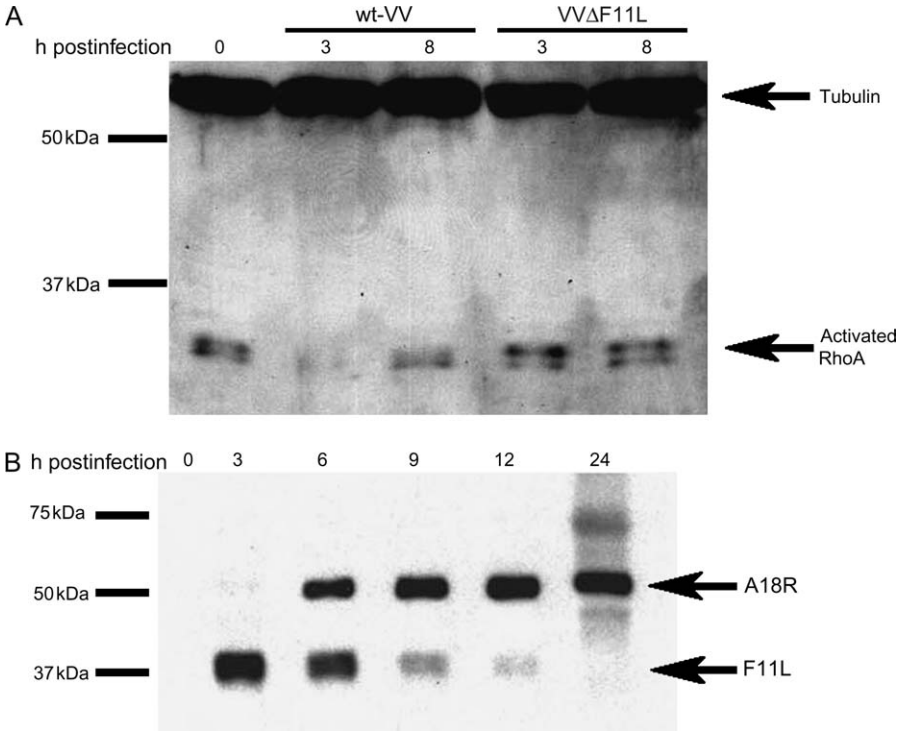

Figure 4: Levels of activated RhoA and F11L expression over the time of infection. In (A), Ptk2 cells were infected or mock infected and lysates prepared as described in *Materials and Methods* and at the indicated times postinfection. Activated RhoA was bound to Rhotekin-RhoA binding domain (RBD) beads and the protein detected by western blotting. Tubulin that bound aspecifically to the beads was used as a loading control. The experiment was repeated four times with the same outcome each time, the blot in (A) showing a representative result. In (B), the expression levels of A18R (used as control) and F11L were analyzed at the indicated times postinfection by western blotting. On the left of the blot in (A) and (B), the position of molecular weight markers is indicated.

body attached to the substrate or to neighboring cells by two to three thin and long actin-rich protrusions [Figure 7C,D; see also Valderrama et al. (16)].

We conclude that F11L is required to modify actin but not microtubules in a way similar to wt-VV. The collective results also imply that the actin modification coincides with directed migration, whereas the collapsed microtubules coincide with contractility.

F11L is not sufficient to induce nocodazole-resistant microtubules

A complementary assay to assess for the microtubular changes that accompanies VV infection is to test for nocodazole-resistant microtubules. Wt-VV infection induces the formation of short microtubular fragments that resist prolonged incubation with high concentrations of nocodazole (11). These tubulin-positive fragments reflect a distinct aspect of the modified microtubular network of wt-VV-infected cells because such fragments are not seen in uninfected or MVA-infected cells (11). Infected cells were therefore incubated with nocodazole before infection and during the infection period and pre-extracted with Triton-X-100 before fixing. This condition revealed multiple short tubulin-positive pieces in wt-VV-infected cells, as seen before [Figure 8A; (11)]. Such fragments were not seen in uninfected (data not shown) or MVA-infected cells and instead a subset of cells displayed several long microtubular filaments that resist prolonged nocodazole treatment (Figure 8E). F11L expression was not required to induce the nocodazole-resistant fragments because they were also very prominent in VVΔF11L-infected cells (Figure 8C) and were not observed in F11L-expressing MVA-infected cells (Figure 8E,G). For quantification, we considered the typical uninfected or MVA-infected phenotype in which cells display either no nocodazole-resistant microtubules or several long filaments as well as the typical wt-VV-infected phenotype with many short tubulin-positive fragments. As shown in Table 1, VVΔF11L-infected cells behaved identical to wt-VV infection because both viruses induced short nocodazole-resistant tubulin fragments in 100% of the infected cells. In contrast, F11L expression in MVA-infected cells did not affect the typical MVA or uninfected pattern, characterized by the complete absence of cells with short tubulin-positive pieces (Table 1).

These data confirm that F11L is not required to modify the microtubular network in a manner seen in cells infected with wt-VV.

VV-induced cellular contractility contributes to the perinuclear accumulation of the viral replication sites

We have previously shown that the perinuclear accumulation of the cytoplasmic sites of VV DNA replication requires intact microtubules (13). Their perinuclear accumulation was dynein independent, and instead, live cell imaging suggested that the motile activities facilitated this process (13). Because F11L was responsible for migration but not contractility, we were now able to directly test whether contractility or migration contributed to their perinuclear accumulation.

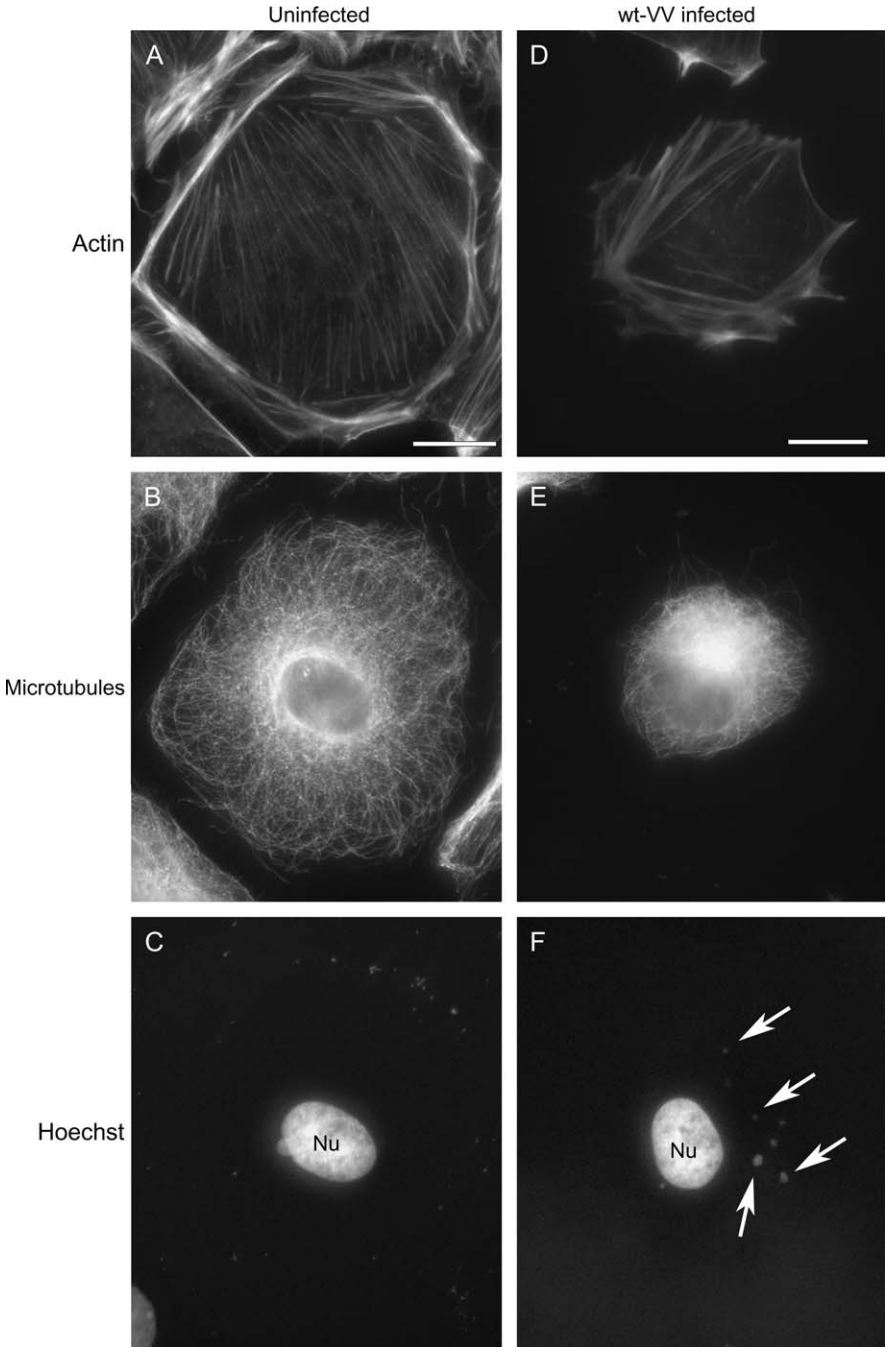

Figure 5: Typical rearrangement of microtubules and actin induced by wt-VV infection. (A–C) are uninfected PtK2 cells and (D–F) infected for 4 h with wt-VV. Cells were fixed with paraformaldehyde and triple labeled with phalloidin–FITC (A and D), anti-tubulin followed by anti-mouse coupled to Cy3 (B and E) and Hoechst (C and F). Uninfected cells show actin fibers that cover the entire cell area (A), whereas in infected cells, they concentrate at the cell borders (D). Microtubules concentrate around the nucleus upon infection (E), whereas in uninfected cells, they extend toward the cellular periphery (B). The Hoechst image shows that infected cells display cytoplasmic Hoechst-positive viral DNA replication sites (arrows in F), typical of this time postinfection. Nu, nucleus. Bars, 10 μm.

Cells were infected for 6 h 30 min, fixed and labeled with anti-H5R, a viral protein that colocalizes with the replication sites. Wt-VV-infected cells displayed large replication sites that were located at the nucleus (Figure 9A), whereas upon MVA infection, they were mostly scattered in the cytoplasm (Figure 9D). GFP-F11L-expressing MVA-infected cells displayed an identical pattern compared with untransfected neighboring cells (Figure 9C,D), implying that F11L expression was unable to induce the perinuclear accumulation of the cytoplasmic replication sites. VVΔF11L-infected cells confirmed this because its replication sites efficiently accumulated around the nucleus (Figure 9B).

Accumulation at the nucleus was quantified by scoring the percentage of cells displaying a phenotype in which more than 90% of the replication sites are at the nucleus (13). As before, upon wt-VV infection, 80–90% of the cells displayed a centered phenotype, and this percentage was very similar in VVΔF11L-infected cells (75–85%). In contrast, MVA-infected cells displayed only 25% centering, and this was independent of F11L expression (Figure 9E).

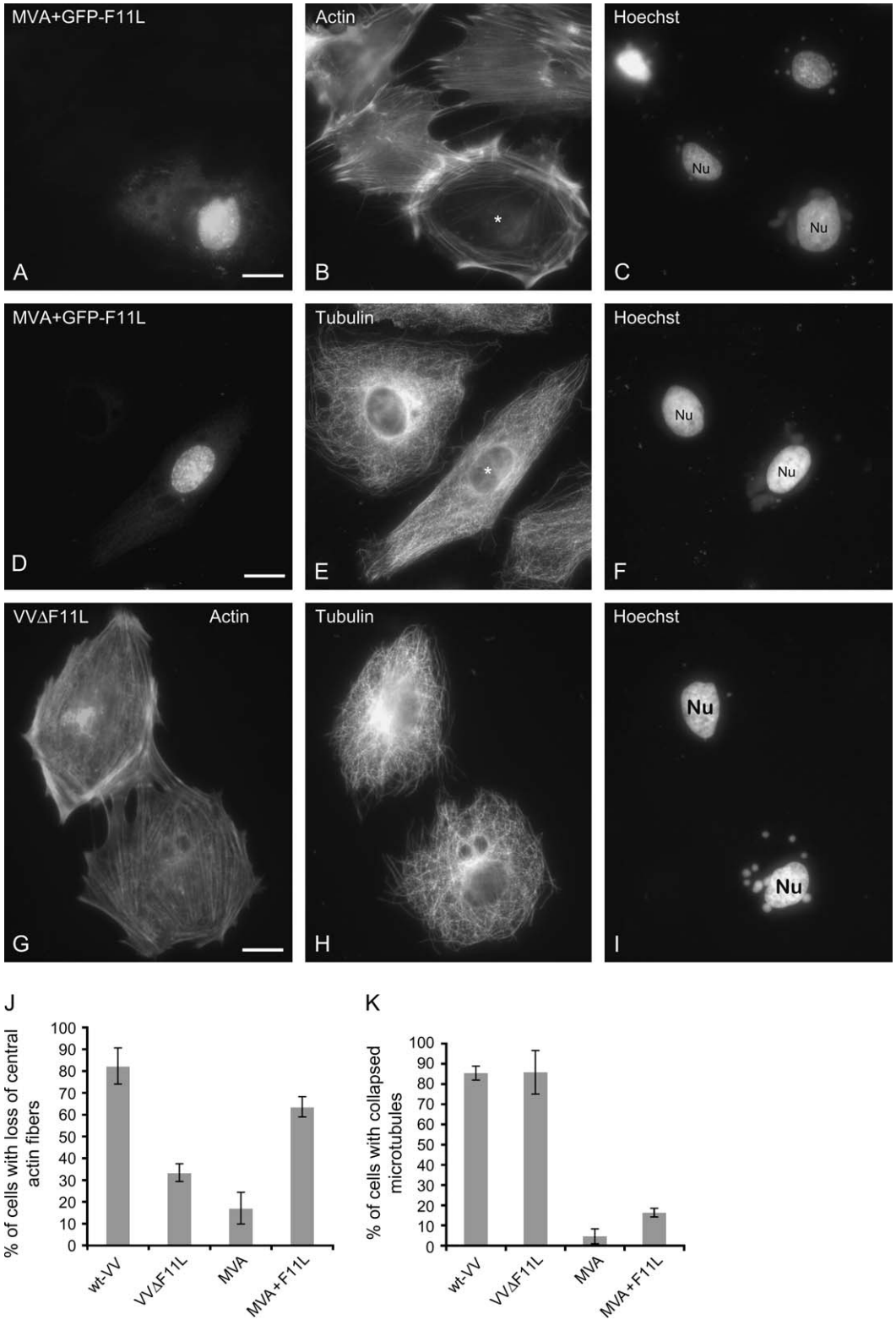

Figure 6: Legend on next page.

The collective data show that F11L is not required for factory centering, and because VVΔF11L infection induces cellular contractility and not migration, the former activity contributes to the perinuclear accumulation of the VV replication sites.

Discussion

Viruses rely entirely on host-cell functions for replication, and infection of cells with viruses provides a powerful system to study cell biological processes in an inducible and synchronized manner. Various steps of the VV life cycle have been shown to interact with both the membranes and the cytoskeleton (*Introduction*). Recent collective data showed that its life cycle also relies on the time-dependent induction of cell motility that consists of contractility and migration and that is accompanied by striking cellular rearrangements (11,13,16). An interesting tool to study the requirements for motility is the attenuated MVA because this virus does not induce motility and cellular changes. Because F11L has recently been implicated in VV-induced migration, we now explored the role of the F11L gene product in the cytoplasmic life cycle of VV, in particular its role in VV-induced motility. We show that F11L is required and sufficient for directed migration but not for contractility. Migration required the rearrangement of actin only, whereas contractility coincided with modified microtubules. We show that the temporal regulation of VV-induced motility may relate to the expression pattern of F11L and RhoA activation during the course of the infection. Finally, we show that contractility contributes to the subcellular distribution of the viral DNA replication sites, whereas migration facilitates cell-to-cell spread of VV.

F11L promotes cell migration

Using siRNA-mediated knockdown, the F11L gene of VV was previously shown to be responsible for VV-induced cell migration as assessed by a wound-healing assay (16). Our study confirms that F11L is essential for VV-induced cell migration; our live cell imaging at intermediate magnification additionally showed that F11L predominantly regulates cell detachment early in infection. Without F11L (VVΔF11L infection), cells were unable to detach, whereas expression of F11L in MVA-infected cells induced their detachment. VVΔF11L-infected cells formed lamellipodia, indicating that part of the process involved in migration was intact in this virus and that the failure to detach was likely to be the main reason for the lack of migration. This observation is consistent with the proposed role of F11L in mediating RhoA inactivation (16). RhoA plays a role in cell adherence and depending on the cell type detachment of the rear of the cell during migration requires activation or inactivation of this GTPase (reviewed in 3). Perhaps, more striking was the observation that F11L seemed to be sufficient to induce migration in MVA-infected cells. It suggests that although MVA-infected cells do not make lamellipodia, the (viral) machinery for migration is intact in MVA, and cell detachment induced by F11L simply allows migration. Alternatively, F11L plays more than just a role in cell detachment, for instance by activating the Rho GTPase rac-1 and CDC42 known to be required to form the leading edge of migrating cells (*Introduction*).

Although F11L seems involved in cell detachment early in infection, live cell imaging of VVΔF11L-infected cells strikingly showed that it plays no role in the establishment of new cell-to-cell contacts late in infection. Thus, although both processes relate to cell adherence, cell attachment seen late in VV infection does not require F11L, suggesting the involvement of a different mechanism.

VV-induced migration coincides with a modified actin network

Our data also show that VV migration coincides solely with the rearrangement of actin, at least at the light microscopy level. Whereas cell migration is known to be accompanied by a dramatic actin remodeling, a regulation of microtubule dynamics is also known to play an important role as well (*Introduction*). Although we did not study the dynamics of microtubules directly in this study, we show that the typical modified microtubule pattern seen early in VV infection (their shortening and resistance of a subset of microtubules to nocodazole) was not required for cell migration. This observation is not at odds with a recent study that concluded that F11L affects microtubule dynamics (17). This study showed that relatively late in infection, a subset of microtubules, those present in the

Figure 6: F11L expression induces actin but not microtubule rearrangements. A–F) PtK2 cells were infected with MVA followed by transfection of GFP-tagged F11L. The cells were fixed at 6-h postinfection to allow sufficiently high expression of F11L and labeled with either phalloidin–rhodamine (B) and Hoechst (C) or anti-tubulin and anti-mouse-Cy3 (E) and Hoechst (F). The F11L-expressing cells (that show GFP signal in the cytoplasm as well as variable amounts in the nucleus) are indicated with an asterisk. F11L expression results in a concentration of the actin pattern at the cell borders (B), whereas the microtubular organization is not affected by the F11L expression (E). G–I) PtK2 cells fixed at 4-h postinfection with VVΔF11L and triple labeled with phalloidin–rhodamine (G), anti-tubulin followed by anti-mouse coupled to FITC (H) and Hoechst (I). The Hoechst labeling in (C), (F) and (I) shows viral DNA replication sites. Nu, nucleus. Bars, 10 μm. (J) and (K) are quantification of the actin (J) and microtubule (K) rearrangements. 'Loss of central stress fibers' indicates cells in which the actin pattern concentrates at the cell borders rather than crossing the entire cell surface (compare Figure 1A with Figure 1D). 'Cells with collapsed microtubules' indicates the pattern in which microtubules concentrate around the nucleus and do not extend into the cellular periphery (compare Figure 1B with Figure 1E). The data were obtained from three independent experiments counting 100 cells per infection condition. The graphs represent the average percentage of cell displaying the defined pattern and standard deviations.

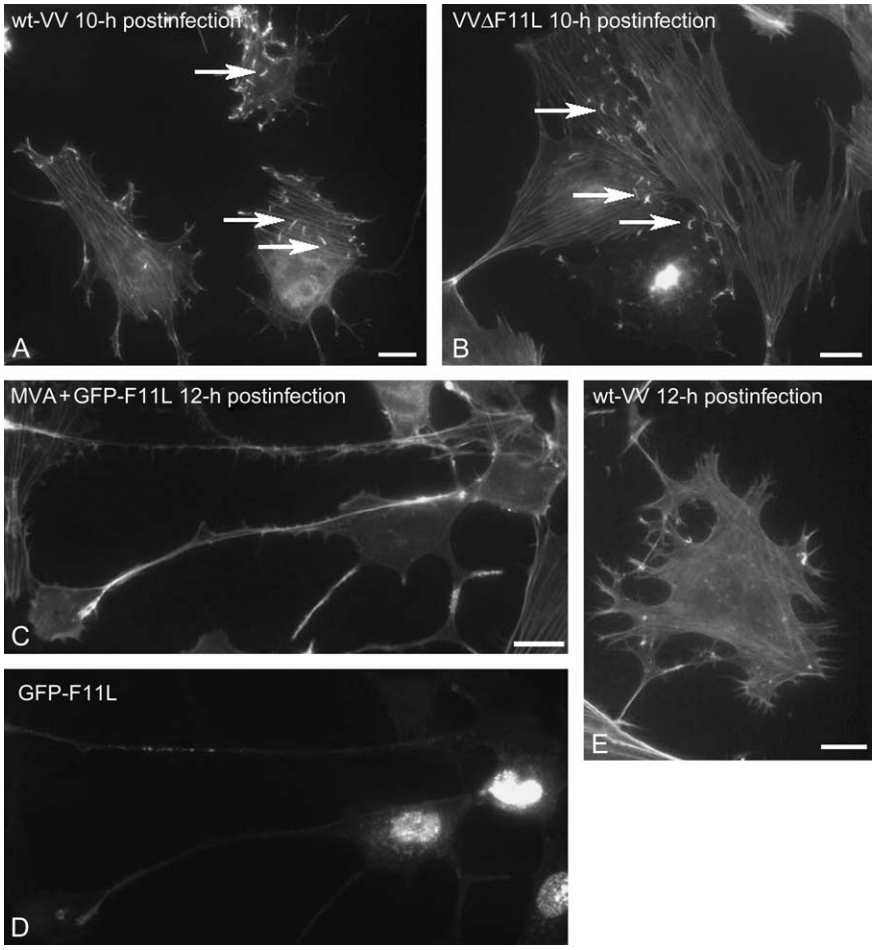

Figure 7: The actin pattern at later times postinfection. PtK2 cells were infected as in Figures 1 and 2, fixed at the indicated times postinfection and labeled with phalloidin–FITC. Wt-VV-infected cells transiently regain central actin fibers (A), reflatten and then adopt a multibranched appearance with thin actin at the cell border (E). In contrast, GFP-F11L-expressing [the GFP-positive cells are shown in (D)] MVA-infected cells round up and form several long projections (C), a morphology that is clearly different from the wt-VV cells at 12-h postinfection (E). VVΔF11L-infected cells display no additional changes to the actin network compared with the early times postinfection (B). The arrows in (A) and (B) indicate actin tails. Bars, 10 μm.

cellular periphery, had an altered dynamics. This time postinfection coincides with cell resettling and cessation of migration, and the altered dynamics of peripheral microtubules could thus reflect these cellular activities rather than migration.

Contractility requires a rearrangement of microtubules

VV motility consists of both migration and contractility, and because both occur at the same time postinfection, we concluded that these two cellular activities underlie the same regulation. Our data now show that both are differentially regulated; cells infected with VVΔF11L showed extensive contractility but no migration, whereas F11L expression in MVA-infected cells predominantly induced migration. Contractility coincided with the typical modified microtubule network consisting of shortened and bundled microtubules that partly resist nocodazole treatment. This wt-VV-induced microtubule phenotype (retraction around the nucleus) is also observed upon overexpression of microtubule-associated proteins, leading to the stabilization of microtubules (22–24). We propose that the retracted microtubules seen upon wt-VV infection reflect a stabilization of the microtubule network, which could provide forces required to induce cellular contractility. Because nocodazole does not completely block contractility, a contribution of the actin network, possibly myosin independent or using yet unidentified myosins, cannot be excluded at present. Cells infected with MVA (no contractility) or with VVΔF11L (contractility) could be used as a model system to understand how cellular contractility is regulated and to what extent microtubules and actin play a role and which signaling pathways are required for this cellular process.

Migration is temporally regulated

We showed before that VV-induced migration occurs early in infection and ceases late in infection (13). Our data now provide a plausible explanation how migration could be temporally regulated. The expression levels of F11L during the course of infection could simply direct migration because F11L is made early in infection, whereas its expression decreases over time. We confirm that F11L expression suppresses activated RhoA, and thus, we propose that the amount of F11L available during the infection could regulate this inactivation and consequently

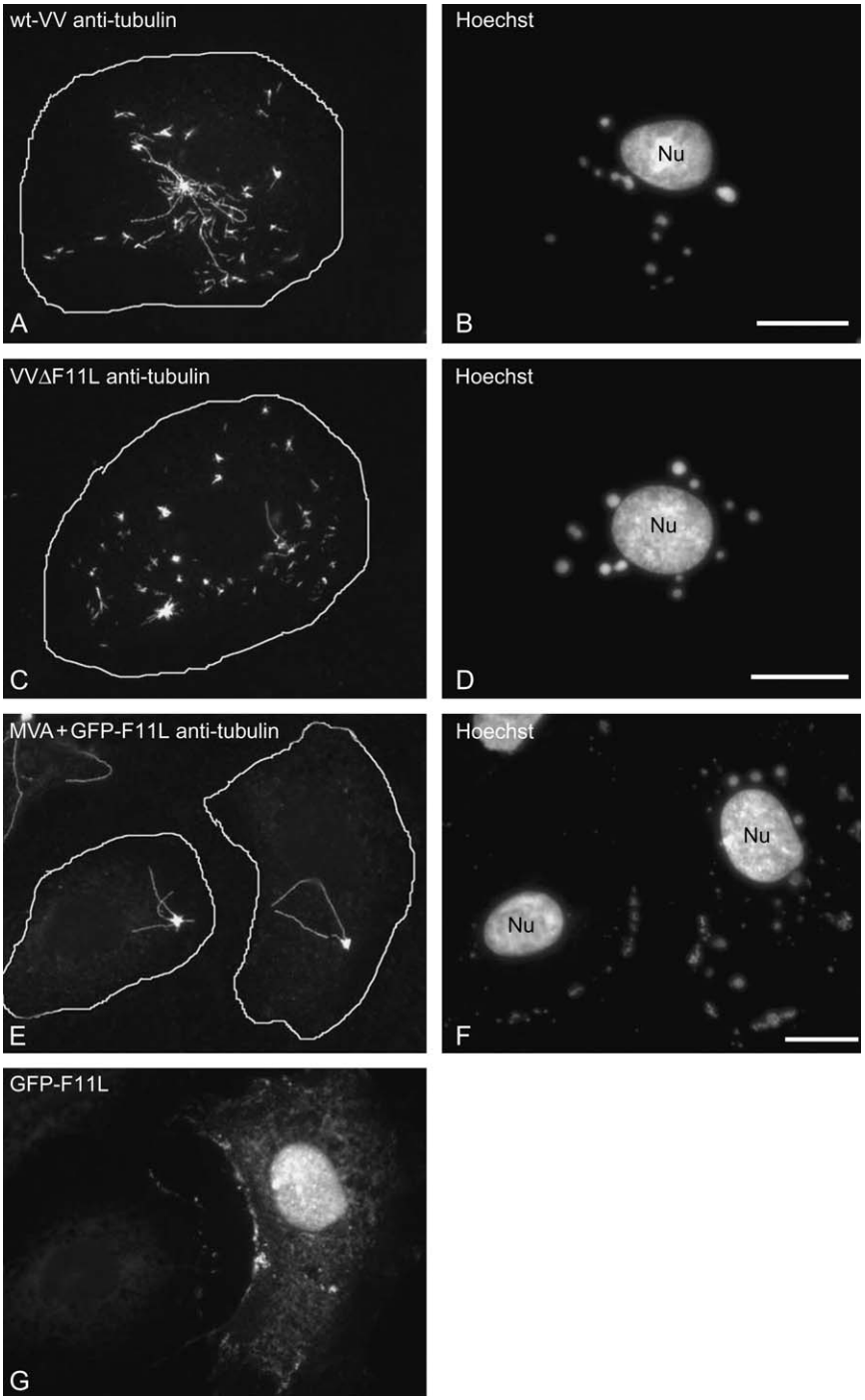

Figure 8: F11L is not required to induce nocodazole-resistant microtubular pieces. PtK2 cells were treated for 30 min on ice with 20 μM nocodazole followed by 30 min of incubation with the drug at 37°C. Cells were then infected in the presence of nocodazole with wt-VV (A and B), VVΔF11L (C and D) or infected with MVA and transfected with F11L-GFP (E–G). At 6-h postinfection, infected cells were incubated for 1 min with 0.1% Triton-X-100 before fixing with 3% paraformaldehyde. Fixed cells were then double labeled with anti-tubulin followed by anti-mouse coupled to Cy3 (A, C and E) and Hoechst (B, D and F). Note that in the presence of nocodazole, the replication sites do not efficiently accumulate around the nucleus. Wt-VV- and VVΔF11L-infected cells display multiple small tubulin-positive fragments in the cytoplasm that are not seen in MVA-infected/F11L-GFP-expressing cells. In (E), the right cell expresses GFP-F11L, while the left cell is untransfected [GFP signal is seen in (G)]. The outlines of the cells are indicated with a white line in (A), (C) and (E). Nu, nucleus. Bars, 10 μm.

regulate migration over time. Whether F11L expression is the sole factor that explains the regulation of RhoA during the infection remains to be established. It is conceivable that F11L exists in an active complex that is disrupted late in infection, resulting in the degradation of the protein. Thus, the assembly and disassembly of this complex would regulate motility rather than the expression levels of F11L. The fact that F11L expression in MVA-infected cells induced cell migration makes it possible to screen for such a putative complex. The latter could regulate cell migration and actin rearrangements in poxvirus-infected cells and could also reveal insights into the regulation of migration in uninfected cells.

Role of F11L in the VV life cycle

In a previous study, we showed that VV-induced contractility correlates with the perinuclear accumulation of the

Table 1: Quantification of cells with nocodazole-resistant microtubular fragments

Infection condition[a]	No fragments[b]	Several long fragments	Many short fragments
Wt-VV (%)	—	—	100
VVΔF11L (%)		—	100
MVA (%)	32.3	67.7	—
MVA + F11L (%)	40.0	60.0	—

[a]PtK 2 cells were pretreated with nocodazole before infection in the presence of nocodazole as described in Figure 7. Cells were fixed at 6-h postinfection after pre-extraction with Triton-X-100 and labeled with anti-tubulin and Hoechst.
[b]Per infection condition, the cells were assigned to three categories; two categories typically occur in uninfected cells or in MVA infected with cells having either no or several long tubulin fragments (Figure 7E), and one category occurs in wt-VV-infected cells displaying many short tubulin-positive fragments after nocodazole treatment (Figure 7A) ($n = 50$).

viral replication sites. We concluded that this cellular activity was apparently accompanied by cytoplasmic forces that were also required to collect the DNA sites at the nucleus (13). This study is consistent with this idea because VVΔF11L-infected cells showed contractility but no migration, while its replication sites efficiently accumulated around the nucleus. We could not confirm a role for F11L virus assembly (16) as shown by the fact that VVΔF11L produced similar amounts of infectious virus in a plaque assay and similar amounts of the different viral forms by EM compared with wt-VV. Our data do, however, show that the lack of F11L reduces the plaque size, implying a role of cell migration in cell-to-cell spread of VV. This observation is interesting in light of the fact that VVΔF11L makes similar amounts of virus-tipped actin tails that have also been implicated in viral cell spread. Whereas a plausible scenario is that both actin tail formation and migration facilitate virus spread, our data underline the importance of migration in this process. The way these two processes are regulated over the time of infection points to highly sophisticated way VV uses the cell for its benefit. Cells are first displaced from their original site of infection, they respread, form new contacts with other cells and then make actin tails to infect their new neighbors.

In brief, our data show that F11L modifies actin and promotes cell detachment to enable cell migration. Contractility coincides with a modified microtubule network and is independent of F11L. The three poxviruses used in this study provide interesting tools to dissect the molecular requirements for cellular contractility and migration and the role of both microtubules and actin play in these processes.

Table 2: Quantification of different viral forms by EM of wt-VV- and VVΔF11L-infected HeLa cells

Viral form[a]	wt-VV	VVΔF11L
IV	11.9 ± 1.1	12.8 ± 1.4
MV	17.9 ± 2.2	15 ± 1.5
IEV	1.8 ± 0.3	1.1 ± 0.2

[a]HeLa cells infected with wt-VV or VVΔF11L were fixed at 8-h postinfection and processed for standard EPON embedding and thin section EM (Figure S1 and Figure 9). Per infection condition, 50 infected cell profiles were considered. The data represent the average and SEM of the three different viral forms (IV, MV and IEV) counted per cell profile.

Materials and Methods

Cells, virus, antibodies and plasmids

PtK2 cells were from American Type Culture Collection and were grown in MEM with 10% heat-inactivated fetal calf serum supplemented with penicillin/streptomycin and glutamine. Purified stocks of wt-VV (strain western reserve), MVA (clone F6 obtained from Dr Gerd Sutter) and VVΔF11L were essentially prepared and titrated as described (11). VVΔF11L was generated by inserting two stop codons at positions G15 (G43T) and Y75 (C225A) following the procedure described by Kato et al. (20). The following antibodies were used throughout this study: rabbit anti-H5R (25), rabbit anti-I3L (26), anti-F11L and anti-A18R (20), anti-alpha tubulin (Sigma) and anti-RhoA (mouse monoclonal clone 55). Phalloidin– fluorescein isothiocyanate (FITC) or rhodamine was from Sigma and used at 0.2 μg/ml. Hoechst (Sigma; #33342) was used at 50 μg/mL to visualize the nucleus and viral replication sites. The F11L gene was amplified from wt-VV DNA by polymerase chain reaction (PCR) using the following primers: 5′-ATAGCGGCCGCGGGTTTTGC-3′ (forward) and 5′GGAATTC*TTA*CAAACG-AAAGTCCAGGTTTG-3′ (reverse). These introduce an *Eco*RI site (underlined) at the 5′ end allowing to clone the F11L gene in frame as a C-terminal fusion to GFP and a *Not*I site (underlined) followed by a stop codon (italics) at the 3′ end. The PCR product was then cloned into the corresponding sites of the pE/L-GFP plasmid (27). Cloning and PCR amplification were verified by sequencing.

Infections, indirect immunofluorescence and quantification

For the plaque assays and the one-step growth curve, BSC40 cells grown in 3.5-cm dishes were infected at a multiplicity of infection (MOI) of 10 for 30 min at 37°C. The cells were harvested at the indicated times post-infection and virus infectivity determined by plaque titration on BSC40 cells. Synchronized infections were done as extensively described in Schepis et al. (11) using sucrose-purified virus stocks. MVA-infected cells were lipofected using Fugene reagent according to the instructions of the manufacturer (Roche Biochemicals). Cells were fixed and processed for indirect immunofluorescence as described (11). Images were taken with a Zeiss Axiovert 200M automated microscope equipped with 1.3 numeric aperture (NA) Planfluar ×40 or ×100 lenses, an Axiocam camera (Zeiss) and acquisition software AXIOVISION (Zeiss). Images were further processed

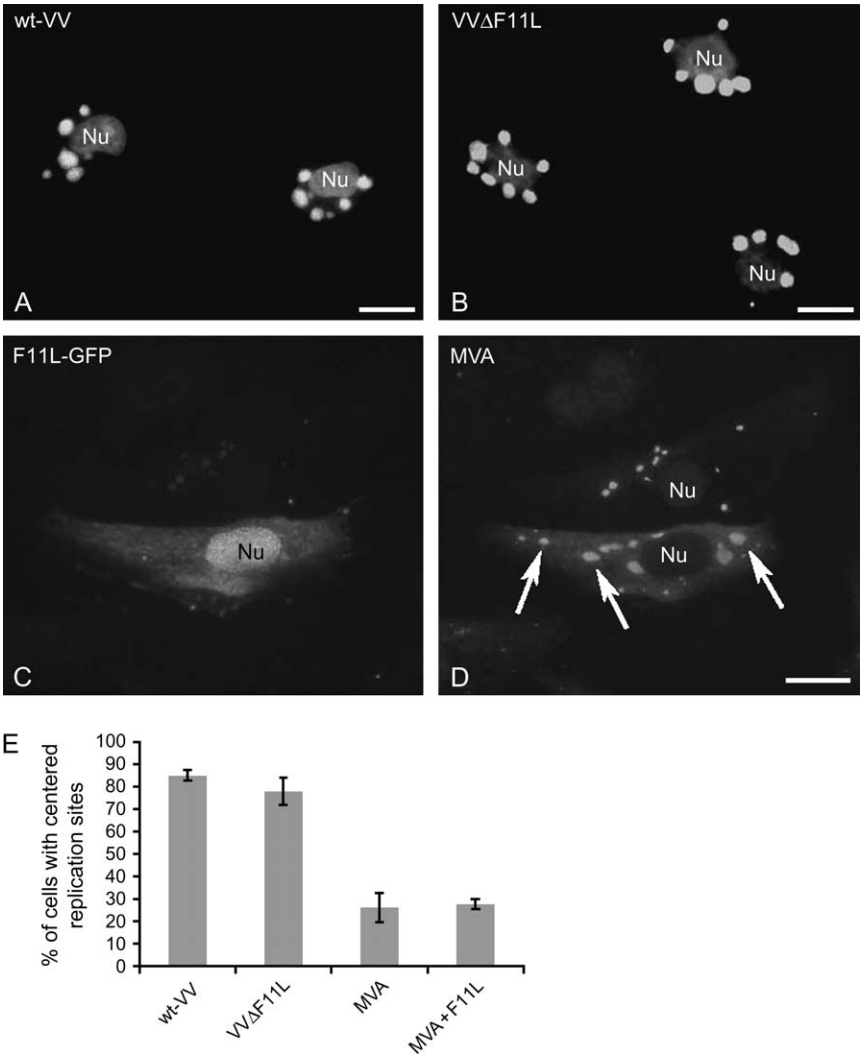

Figure 9: F11L expression is not required for the accumulation of the viral replication sites around the nucleus. PtK2 cells were infected with wt-VV, VVΔF11L and MVA transfected with F11L-tagged GFP. Cells were fixed at 6.30-h postinfection, the time required for the viral replication sites to accumulate around the nucleus. Fixed cells were labeled with anti-H5R followed by anti-rabbit coupled to Cy3. Whereas in wt-VV-infected cells (A) and VVΔF11L-infected cells (B), the replication sites are at the nucleus in MVA-infected cells [(C and D), replication sites are indicated with arrows in (D)], they remain distributed over the cytoplasm. Nu, nucleus. Bars, 10 μm. In (E), the percentage of cells displaying a pattern in which more than 90% of the replication sites are at the nucleus (centered phenotype) was quantified. The data were obtained from 100 cells per condition and from three independent experiments.

using ADOBE PHOTOSHOP. Quantification of the actin and microtubular patterns were done at 4 h of wt-VV and VVΔF11L infection but 6 h after MVA infection. When expressed from a synthetic early/late promoter, expression of the protein is detected from about 4-h postinfection onwards only and thus somewhat later than during a wt-VV infection. This necessitates slightly longer infection/expression times with MVA-infected F11L-expressing cells. For all quantitative experiments, the results were obtained from three independent experiments counting 50–100 cells per experiment and per condition. The pre-extraction with Triton-X-100 before fixing was essentially carried out as described by Schepis et al. (11). For the quantification of actin tails, PtK2 cells were infected with either wt-VV or VVΔF11L and fixed with 3% paraformaldehyde at 8-h postinfection. After labeling with phalloidin–FITC, 100 cells were considered displaying either actin tails (as shown in Figure 7A,B) or not.

Live cell imaging

Live cell imaging was carried out as described by Schramm et al. (13). Ptk2 cells were grown on glass bottom culture dishes (MatTek) and infected as described above. Cells were imaged using a DeltaVision restoration microscope (Applied Precision, LLC), and a time-lapse analysis of the cells was performed using an LC PlanFl ×20 lens with a 0.4 NA (Olympus). Image acquisition corresponding to a 1024 × 1024 imaging field was done using the SOFTWORX program. For GFP-F11L-transfected Ptk2 cells, a dualband-filterset EGFP/DsRed filter was used. Frames of 10 different positions were taken every 8 min for a total period of 12–20 h. Preparation of the final movies was done using the SOFTWORX SUITE software.

Electron microscopy

HeLa cells were infected with wt-VV or VVΔF11L at an MOI of 10 and fixed for epoxy resin (EPON) embedding at 8-h postinfection. EPON embedding and thin sectioning were as described by Griffiths (28). Per condition, the total amount of IVs, MVs and IEVs were counted and the average of these viral forms per infected cell profile estimated.

Western blots and RhoA-GTP pull-down experiments

Western blots of F11L and A18R were essentially as described (20). For RhoA pull-down experiments, cells grown in 15-cm dishes were mock infected or infected with wt-VV or VVΔF11L in serum-free medium at an MOI of 10. At 3- and 8-h postinfection, cells were washed with ice-cold PBS and scraped and lysed in 750 μL RhoA-binding buffer (50 mM Tris–Cl, pH 7.5, 10 mM MgCl2, 300 mM NaCl and 2% Nonidet P-40) containing protease inhibitors. After centrifugation for 2 min to remove nuclei, 50 μL was taken for direct analysis to detect the total amounts of RhoA, tubulin (as a loading control) and the VV protein I3L (as a control for infection) in the lysate. The rest of the supernatant was incubated for 60 min at 4°C

by end-over-end rotation with 60 μL of Rhotekin-RhoA binding domain (RBD) protein glutathione S-transferase beads (Cytoskeleton). Beads were spun down for 1 min at 6000 r.p.m. and washed once with RhoA wash buffer (25 mM Tris–Cl, pH 7.5, 30 mM MgCl2 and 40 mM NaCl) before resuspending in sample buffer. Bound, activated RhoA was detected by western blotting using anti-RhoA monoclonal antibody (clone 55) and anti-tubulin as a loading control.

Acknowledgments

We thank Sabrina Marion and Gareth Griffiths for critical reading of the manuscript. This study was supported by grants from the EU fifth framework to J. K. L., Conselho Nacional de Desenvolvimento Científico e Tecnológico, Brazil (CNPq) and Fundação Carlos Chagas Filho de Amparo a Pesquisa do Estado do Rio de Janeiro (FAPERJ) to N. M. N. M. and F. A. B. G. were recipients of fellowship from CNPq, and S. E. M. K. was recipient of fellowships from CAPES and CNPq.

Supplementary Materials

Figure S1: Assembly of wt-VV and VVΔF11L by EM. Cells were infected with wt-VV and VVΔF11L and fixed at 8-h postinfection, embedded in EPON and sectioned. The figure shows that both viruses produce all viral forms; these are the spherical IV and MVs that undergo wrapping by Golgi membranes [for example, in (E–G)] to become IEVs. E, endosomes; GC, Golgi complex; Nu, nucleus.

Movie S1: Live cell imaging of wt-VV-infected PtK2 cells. PtK2 cells grown in microscopy dishes were infected with wt-VV and imaged from 1 h 13 min- to 12 h 11 min postinfection with 8-min intervals between frames using a ×20 lens. It shows how cells detach early in infection, undergo phases of contraction and directed migration. Late in infection, cells reflatten, adopt a multibranched appearance and stop moving.

Movie S2: Live cell imaging of MVA-infected PtK2 cells. PtK2 cells were infected with MVA and imaged from 0.59- to 12-h postinfection with 8-min intervals between frames. In great contrast to wt-VV-infected cells, no obvious contractility or migration is observed during the recorded period.

Movie S3: Live cell imaging of MVA-infected cells expressing GFP-F11L. PtKs cells were infected with MVA and transfected with pE/L-GFP-F11L. Imaging was from 1.17- to 20-h postinfection with 8-min intervals between frames. From about 4-h postinfection onwards, GFP-expressing cells can be detected. These GFP-positive cells are seen to undergo various activities; three of them (one in top right, one in top left and one in bottom right) move through the monolayer, the bottom cells leaving the field of view. Late in infection, expressing cells round up and form long thin protrusions. The cell that moves from the top right seems to use these protrusions to attach to and detach from neighboring cells. In this movie, three cells that do not express F11L round up and apparently die relatively early in infection that is caused by the infection/transfection and is not seen upon MVA infection only. Some of the main features of this movie are shown in the still images in Figure 1.

Movie S4: Live cell imaging of PtK2 cells infected with VVΔF11L. Imaging was 1.04- to 12-h postinfection with 8-min intervals between frames. It shows how early in infection infected cells undergo extensive phases of blebbing and contractions. One cell forms a lamellipodium but is unable to detach from its neighbor. Later, the extensive phases of contractions cease and cells start growing protrusions with which they eventually establish contact with neighboring cells. Representative events are shown in sequences of still images in Figure 2.

Supplemental materials are available as part of the online article at http://www.blackwell-synergy.com

References

1. Wittmann T, Waterman-Storer CM. Cell motility: can Rho GTPases and microtubules point the way? J Cell Sci 2001;114:3795–3803.
2. Raftopoulou M, Hall A. Cell migration: Rho GTPases lead the way. Dev Biol 2003;265:23–32.
3. Ridley AJ. Rho GTPases and cell migration. J Cell Sci 2001;114:2713–2722.
4. Watanabe T, Noritake J, Kaibuchi K. Regulation of microtubules in cell migration. Trends Cell Biol 2005;15:76–83.
5. Rodriguez OC, Schaefer AW, Mandato CA, Forscher P, Bement WM, Waterman-Storer CM. Conserved microtubule-actin interactions in cell movement and morphogenesis. Nat Cell Biol 2003;5:599–609.
6. Small JV, Geiger B, Kaverina I, Bershadsky A. How do microtubules guide migrating cells? Nat Rev Mol Cell Biol 2002;3:957–963.
7. Etienne-Manneville S. Actin and microtubules in cell motility: which one is in control? Traffic 2004;5:470–477.
8. Basu R, Chang F. Shaping the actin cytoskeleton using microtubule tips. Curr Opin Cell Biol 2007;19:88–94.
9. Schramm B, Krijnse Locker J. The cytoplasmic organization of Poxvirus DNA-replication. Traffic 2005;6:839–846.
10. Moss B, Ward BM. High-speed mass transit for poxviruses on microtubules. Nat Cell Biol 2001;3:E245–E246.
11. Schepis A, Schramm B, De Haan CM, Krijnse Locker J. Vaccinia virus induced microtubule-dependent cellular rearrangements. Traffic 2006; 7:308–323.
12. Sanderson CM, Way M, Smith GL. Virus-induced cell motility. J Virol 1998;72:1235–1243.
13. Schramm B, de Haan CM, Doglio L, Schleich S, Reese C, Popov A, Steffen W, Schroer TA, Krijnse Locker J. Vaccinia virus induced cellular contractility facilitates the sub-cellular localization of the viral replication sites. Traffic 2006;7:1352–1367.
14. Carroll MW, Moss B. Host range and cytopathogenicity of the highly attenuated MVA strain of vaccinia virus: propagation and generation of recombinant viruses in a nonhuman mammalian cell line. Virology 1997;238:198–211.
15. Drexler I, Heller K, Wahren B, Erfle V, Sutter G. Highly attenuated modified vaccinia virus ankara replicates in baby hamster kidney cells, a potential host for virus propagation, but not in various human transformed and primary cells. J Gen Virol 1998;79:347–352.
16. Valderrama F, Cordeiro JV, Schleich S, Frischknecht F, Way M. Vaccinia virus-induced cell motility requires F11L-mediated inhibition of RhoA signaling. Science 2006;311:377–381.
17. Arakawa Y, Cordeiro JV, Way M. F11L-mediated inhibition of RhoA-mDia signaling stimulates microtubule dynamics during vaccinia virus infection. Cell Host Microbe 2007;1:213–226.
18. Moss B. Poxviridae: the viruses and their replication. In: Fields BN, Knipe DM, Howley PM, Chanock RM, Hirsch MS, Melnick JL, Monath TP, Roizman B, editors. Fields Virology, 4th edn. Philadelphia: Lippincott-Raven Press; 2001, pp. 2849–2883.
19. Rabut G, Ellenberg J. Automatic real-time three-dimensional cell tracking by fluorescence microscopy. J Microsc 2004;216:131–137.
20. Kato SE, Greco FA, Damaso CR, Condit RC, Moussatche N. An alternative genetic method to test essential vaccinia virus early genes. J Virol Methods 2004;115:31–40.
21. Doglio L, De Marco A, Schleich S, Roos N, Krijnse Locker J. The Vaccinia virus E8R gene product; a viral membrane protein that is made

early in infection and packaged into the virions' core. J Virol 2002;76: 9773–9786.
22. Bulinski JC, McGraw TE, Guber D, Nguyen HL, Sheetz MP. Overexpression of MAP4 inhibits organelle motility and trafficking in vivo. J Cell Sci 1997;110:3055–3064.
23. Ebneth A, Godemann R, Stamer K, Illenberger S, Trinczek B, Mandelkow EM, Mandelkow E. Overexpression of tau protein inhibits kinesin-dependent trafficking of vesicles, mitochondria, and endoplasmic reticulum – implications for Alzheimers-disease. J Cell Biol 1998; 143:777–794.
24. Lee G, Rook SL. Expression of tau protein in non-neuronal cells: microtubule binding and stabilization. J Cell Sci 1992;102:227–237.
25. Tolonen N, Doglio L, Schleich S, Krijnse Locker J. Vaccinia virus DNA-replication occurs in ER-enclosed cytoplasmic mini-nuclei. Mol Biol Cell 2001;12:2031–2046.
26. Welsch S, Doglio L, Schleich S, Krijnse Locker J. The vaccinia virus I3L gene product is localized to a complex endoplasmic reticulum-associated structure that contains the viral parental DNA. J Virol 2003;77: 6014–6028.
27. Frischknecht F, Moreau V, Rottger S, Gonfloni S, Reckmann I, Superti-Furga G, Way M. Actin-based motility of vaccinia virus mimics receptor tyrosine kinase signalling. Nature 1999;401:926–929.
28. Griffiths G. Fine Structure Immunocytochemistry. Heidelberg: Springer Verlag; 1993.